RSC Advances

ROYAL SOCIETY OF CHEMISTRY

www.rsc.org/advances

RSC Advances

ARTICLE

Thermosensitivity profile of malign glioma U87-MG cells and human endothelial cells following γ-Fe_2O_3 NPs internalization and magnetic field application

Received 00th January 20xx,
Accepted 00th January 20xx

DOI: 10.1039/x0xx00000x

www.rsc.org/

A. Hanini,[a,b,c] L. Lartigue,[d] J. Gavard,[b] A. Schmitt,[b] K. Kacem,[c] C. Wilhelm,[d] F. Gazeau,[d] F. Chau[a] and S. Ammar[a,†]

In this study we evaluate the thermosensitivity of healthy endothelial cells (HUVEC) and malign gioblastom (U87-MG) to magnetic hyperthermia (ac-magnetic field of 700 kHz, 23.10 kA.m^{-1}) for 1 hour with and without the presence of superparamagnetic 10 nm sized polyol-made γ-Fe_2O_3 nanoparticles (NPs). Interestingly, despite their reduced size, NPs exhibit a high magnetization, close to that of the bulk material, in relation with their high crystalline quality. In practice, they ensured an efficient heating capacity, leading to about 20 % and more than 50 % cell death of HUVEC and U87-MG lines, respectively, when hyperthermia assays were achieved in presence of these NPs. Magnetophoresis and X-Ray fluorescence spectrometry measurements evidenced a more important internalization of NPs in U87-MG than in HUVECs. Surprisingly both cell lines reached the same maximal temperature, namely 42°C, after hyperthermia treatment suggesting a higher thermosensitivity of the former compared to the latter, establishing the fact that polol-madeγ-Fe_2O_3 NPs assisted hyperthermia is a harmful agent to glioma treatment.

Introduction

Magnetic hyperthermia is based on injection of magnetic nanoparticles (NPs) as an aqueous suspension (Magnetic Fluid Hyperthermia or MFH) on identified site such as tumor site. By applying an external alternative magnetic field, NPs generate heat through oscillation of their magnetic moment due to Néel relaxations and/or through friction between their whole moving core and their fluid career. [1] As a result the tumor temperature increased selectively and uniformly, causing cell death by apoptosis and/or necrosis. [1] Considering the therapeutic benefit of such original approach, worldwide interest in hyperthermia treatment is on the rise. Several studies have been carried out to tentatively improve the magnetocalorimetric response of the magnetic NPs, varying their nature, ferromagnetic metals [2] or ferrimagnetic oxides, [3] their size, small or large, [4] their aggregation state [5] and finally their shape. [6] But among all the considered materials, almost isotropic in shape nanometer-sized iron oxide remains the most studied system [7] since it is considered as relatively safe at reasonable doses. Iron is one of the most abundant transition metal in human body (the average adult possessing ca. 5 g). Moreover, acting on its material processing conditions, one can tune its microstructural properties, particularly its particle crystalline quality, and then its heating capability. Even experiments were elaborated with iron oxide NPs of different sizes, various surface coating, produced by numerous synthesis routes (see for instance reference [1,4,7,8]), little is known about the efficiency of polyol-made ones for hyperthermia application. [9-11] To the best of our knowledge, the main results concern large monocrystalline iron oxide, [9] highly anisotropic ultrafine cobalt ferrite oxide [10] or richly zinc substituted ferrite ones. [11] Generally speaking it has been shown that polyol process generates monodispersed NPs with high crystalline quality. [9-12] These characteristics are usually prerequisite for the efficiency of magnetic hyperthermia application. In this context we focused our investigations on the heating capability of 10 nm sized maghemite NPs produced by the polyol process [12] when delivered into two kind of human cell lines, healthy endothelial cells (HUVEC) and malign glioma (U87-MG) ones, at a reduced concentration (50 µg.mL^{-1} in serum-free DMEM cell culture medium). Indeed, even if *in vitro* magnetic fluid hyperthermia on healthy cells was frequently considered, [13] studies on endothelial cells from the microvasculature such as HUVECs are poorly documented. Moreover, even if many attentions have been made on glioblastoma cells because of their high malignancy, [14] hyperthermia investigation on U87-MG cell lines remains scarce.

Experimental

Iron oxide NPs

10 nm sized maghemite particles were prepared according to a protocol previously described. [15] Typically, $Fe_{3-x}O_4$ NPs were obtained by forced hydrolysis of iron acetate salt in diethylene-glycol. They were then recovered by ultra-centrifugation and finally washed by hot water to be oxidized as γ-Fe_2O_3. [16] These particles are almost monodisperse (standard size deviation of 10%) and well-crystallized within the spinel structure as evidenced by Transmission Electron Microscopy (TEM) (Figure 1). The surface of NPs is almost free. Only a few organic content (C: 1.8 wt.-% ; H: 0.2 wt-%) corresponding to some synthesis residues, mainly

[a] ITODYS, Université Paris Diderot, SPC, CNRS UMR-7086, Paris, France.
[b] Institut Cochin, Université Paris Descartes, SPC, CNRS UMR-8104, Paris, France.
[c] LPI, Faculté des Sciences de Bizerte, Université de Carthage, Zarzouna, Tunisia.
[d] MSC, Université Paris Diderot, SPC, CNRS UMR-7057, Paris, France.
† Corresponding author: ammarmer@univ-paris-diderot.fr

acetate, is shown by FTIR spectroscopy (Figure 2).

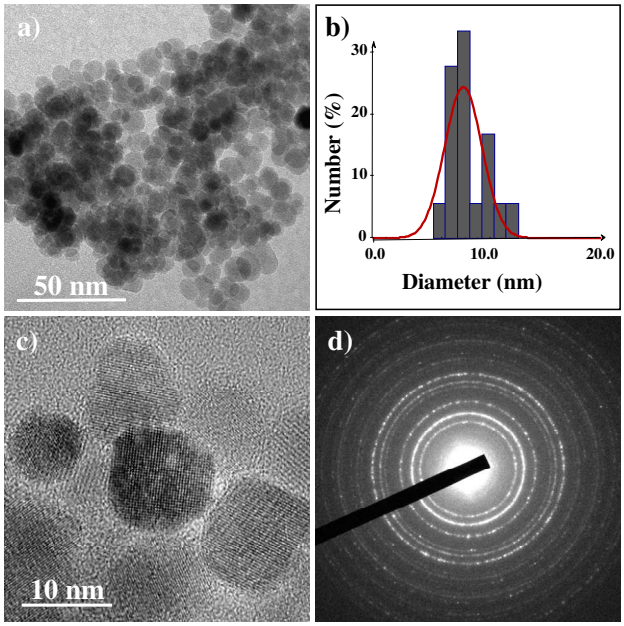

Figure 1. TEM image of an assembly of NPs, recorded with a JEOL 2100F microscope (a). Their size distribution, as inferred from the statistical analysis of 200 objects assumed to be spheres using SAISAM software (Microvision) (b). High resolution TEM micrograph of some representative particles (c) and their electron diffraction pattern which is well-consistent with the spinel structure (d).

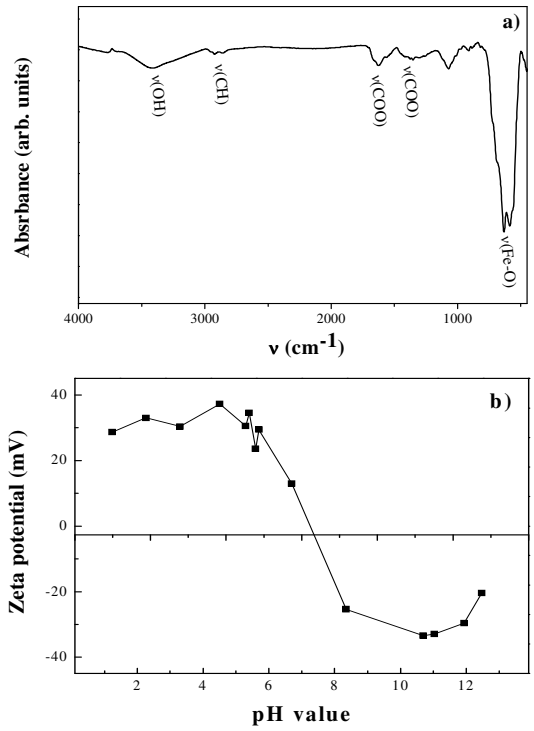

Figure 2. FTIR spectrum of the as-produced NPs, recorded on a BRUKER Equinos spectrometer (a). Zeta potential of their aqueous suspension measured as a function of the pH using a Nanosizer Malvern instrument (b).

As a consequence, their isoelectric point, when dispersed in water, is close to pH = 7. They are positively charged below this pH and negatively charged above it (Figure 2).

Finally, their magnetic properties were investigated using a Quantum Design MPMS-5S SQUID magnetometer. In practice, the field-dependent magnetization was measured at body temperature (+37°C) in the -50 kOe to +50 kOe (namely 33675.58 kA.m^{-1}), magnetic field range on a given mass of particles, slightly compacted in a diamagnetic plastic sampling tube to avoid their displacement during experiments. The thermal variation of their dc-susceptibility was also collected under a magnetic field of 200 Oe (namely 134.30 kA.m^{-1}), in the 5 - 325 K temperature range, in both field cooling (FC) and zero-field cooling (ZFC) modes.

HUVEC and U87-MG cells

Immortalized human umbilical vascular endothelial cells (HUVECs) Ea.hy 926 clone [17] and Human glioblastoma cell line formally known as U87-MG (cells were obtained from a stage three cancer patient). [18] HUVECs and U87-MG cells were maintained in Dulbecco's Modified Eagle Medium (DMEM) supplemented with 10% fetal bovine serum (FBS) and 100 µg.mL^{-1} streptomycine and 100 U.mL^{-1} penicillin (Gibco, Invitrogen, Cergy-Pontoise, France) at +37°C in a humidified atmosphere with 5% CO_2.

NPs incubation with cells and cell viability determination

About five thousands cells were cultured, separately, overnight onto 96-well plates. After quick ultra-sonication in serum-free DMEM, γ-Fe_2O_3 NPs were added to reach different concentrations (typically, 50 and 100 µg.mL^{-1}). Cells were then incubated by this solution for 4 hours, and then washed 3 times. To evaluate their cell viability, MTT assays were then performed, according to manufacturer's instructions (Sigma, France). [15] The results were expressed as normalized cell viability, calculated as a ratio between sample and control, the control corresponding to non-incubated cells. Note, an automate was used to determine cell viability.

Quantification of internalized NPs

To determine the exact amount of internalized NPs into the cells for a given NP incubation dose, magnetophoresis and X-ray Fluorescence Spectroscopy (XRF) were performed. Magnetophoresis consists of measuring the magnetization of a cell after NPs incubation (and hence the number of internalized particles inside it) by following its migration along a constant magnetic field gradient (grad[B] = 17 T.m^{-1}, B = 145 mT). From video footage, the diameter (d_{cell}) and velocity (v_{cell}) of the cells towards the magnet were measured in a given fluid of η viscosity, leading to the determination of the magnetisation per cell (M_{cell}) by balancing the magnetic (F_{mag} = M_{cell} grad[B]) and the viscous drag (F_{vis} = $3\pi\eta d_{cell} v_{cell}$) forces acting on it. NPs quantified into the cell, usually expressed as iron mass (in pictogram: pg), can be then calculated using the following equation: [19]

$$m_{Fe} = \frac{M(Fe_2)}{M(Fe_2O_3)} \frac{\rho}{M_v} M$$

where m_{Fe} measures the mass of iron, $M(Fe_2O_3)$ and $M(Fe_2)$ correspond to the molar mass of the Fe_2O_3 iron oxide and the Fe_2 iron contribution in the studied magnetic NPs, respectively, ρ the density of the maghemite phase, namely 4.90 g.cm^{-3}, M_v the

particle magnetization (a magnetic moment of 6.60 10^{-14} A.m² corresponds to 1 pg of iron, 1 10^6 were analysed per sample).

XRF experiments were also performed to determine the amount of internalized NPs in each kind of cell line, by analyzing its iron content. Typically, all the incubated cells were mineralized in 350 µL of nitric acid and 150 µL of hydrochloric acid during 48 hrs at room temperature (+25°C). 50 µL of each resulting solution were then deposited on a clean cellulose membrane and analyzed by a MINIPAL4 XRF spectrometer equipped with a rhodium X-ray tube operating at 30 kV and 87 µA current emissions. The iron content was determined by comparing the collected iron XRF intensity signal to that of certified iron solutions with appropriate compositions. The results were expressed in mass of iron in pg.

Magnetic hyperthermia experiments

Magnetocalorimetric measurements were performed with a laboratory-made device, described in previous works. [20] It consists of a resonant RLC circuit producing in a 16 mm diameter thermalized at +37°C coil operating at 700 kHz magnetic field with an amplitude of 34.4 Oe (namely 23.10 kA.m^{-1}). The temperature was probed with a fluoro-optic thermometer in a 300 µL of the sample. The sample corresponds to i) NPs dispersed in distilled water (20 g.L^{-1}), ii) free cells (~10^6) in DMEM or iii) NPs incubated (50 µg.mL^{-1}) cells (~10^6) cultured in DMEM. In all the cases, the sample was stirred before the measurement to avoid potential precipitation. The initial slope of the curve temperature T as a function of time t was measured in order to deduce the specific absorption rate (SAR) of the NPs: [21]

$$SAR = \frac{CV_s}{m}\left(\frac{dT}{dt}\right)_{t=0}$$

Where C, V_s and m correspond to the volume specific heat capacity of water (C = 4185 J.L^{-1}.K^{-1}), the sample volume (fixed to 300 µL in the used hyperthermia setup) and the mass of iron oxide NPs.

In practice, ~10^6 cells were incubated with 50 µg.mL^{-1} of γ-Fe_2O_3 NPs in serum free culture medium during 4 hours at +37 °C. The incubated cells were then submitted to the ac-magnetic field for 1 hour. The same experiment was carried out on free cells to serve as a control for each cell line. Immediately following hyperthermia application, samples cell series were labeled by propidium iodide (PI) to identify death cell and count them. PI is commonly used for identifying dead cells in a population and acts as a counter stain in multicolor fluorescent techniques. [22] PI was purchased from Sigma-Aldrich (95%) and used without further purification. Typically, 10 µL of PI iodide salt were added to cells and leaved for about 10 min at room temperature. Then cells were carried up on slide and coverslip, and observed using an inverse microscope (Leica DM IRB, Solms, Germany) coupled to a high sensitive CCD-camera (CoolSNAP, Photometrics, Tucson, Arizona, USA). Cells were counted using Image-J software.

Transmission Electron microscopy (TEM) was also carried out on the treated cells to follow their morphology evolution. In practice, the cells were washed with 0.10 M pH 7.20 sodium cacodylate buffer, then processed for TEM. They were first mixed to 3% glutaraldehyde/0.10 M pH 7.20 in a sodium cacodylate buffer for 30 min at room temperature. They were then incubated in 1% OsO_4 and finally dehydrated in graded dilutions of ethanol to be subsequently embedded in artificial resin (Epon) from which ultrathin slices were cut. The cell ultrastructure was analyzed by a EM10CR, Zeiss TEM microscope operating at 60-80 kV on unstained thin sections.

Note, all experiments were repeated thrice. Data were analyzed using one-way analysis of variance (ANOVA) followed by unpaired Student t-test. Values are expressed as mean plus standard deviation SD p values of <0.05 were considered statistically significant.

Results

Magnetic and magnetocalorimetric properties of free γ-Fe_2O_3 NPs

The thermal variation dc-magnetic susceptibility χ(T) of the produced iron oxide particles measured in both zero Field cooling and field cooling conditions was plotted in Figure 3.

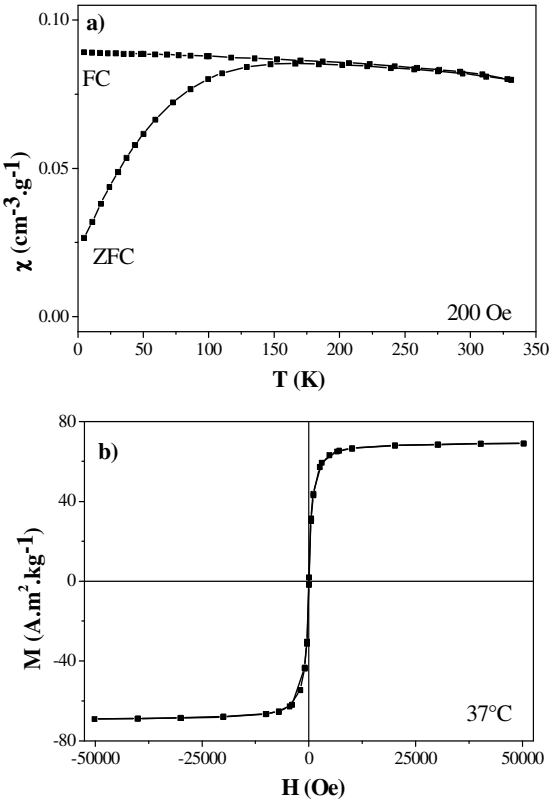

Figure 3. The FC and ZFC thermal variation of the dc-magnetic susceptibility of the as-produced γ-Fe_2O_3 NPs (a) and their hysteresis loop measured at 37°C (b).

The obtained curves are typical of single magnetic domains exhibiting a superparamagnetic behavior. Typically, a net irreversibility between the ZFC and FC branches is observed below a critical temperature called the blocking temperature T_B which is found here to be about 175 K (measured at the maximum of the ZFC plot). T_B represents the threshold temperature above which magnetic anisotropy barrier is overcome by thermal activation energy solely. The magnetization M variation vs magnetic field H measured at

body temperature is also depicted in Figure 3. It confirms the superparamagnetic behavior of the produced NPs since neither coercivity nor remanence appear in the plotted loop. The reached magnetization at a magnetic field as high as 50 kOe is found to be 69 $A.m^2.kg^{-1}$, close to that of bulk maghemite in agreement with their expected high crystalline quality.

Magnetocalorimetry measurements were also performed on the as-produced particles when just dispersed in distilled water (20 $g.L^{-1}$), using a home-made hyperthermia steup. [16] Applying a 700 kHz ac-magnetic field, the temperature increase of the resulting aqueous suspension as a function of time is plotted in Figure 4. It appears that the recorded highest temperature after application of alternative field reaches rapidly a value of 58°C, far from the desired therapeutic 41-45°C values, evidencing the ability of these NPs to generate efficient heating. The initial linear rise in temperature versus time dependence, dT/dt, was thus determined by a linear fit of the data and used to calculate the SAR of the NPs. A value of 84 ± 10 $W.g^{-1}$ was found, which is remains quite comparable to the values reported by dfferent authors on almost smiliarly sized maghemite particles prepared by various routes. [23]

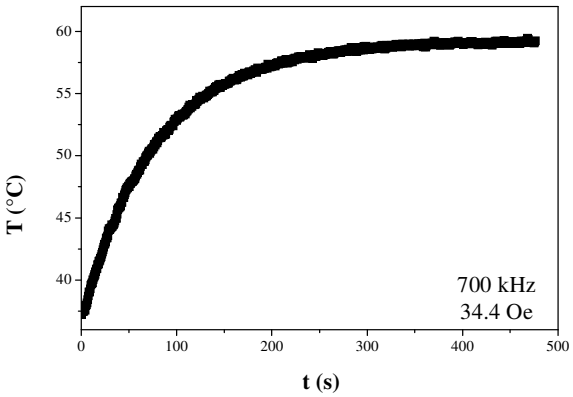

Figure 4. Magnetically-induced temperature increase plotted as a function of time, measured on an aqueous suspension of γ-Fe_2O_3 NPs, after application of 700 kHz ac-magnetic field.

Magnetocalorimetric properties of incubated HUVEC and U87-MG cells

Both healthy HUVECs and malign U87-MGs where incubated for 4 hours with 50 $\mu g.mL^{-1}$ NPs doses. The particle exposure time and doses were inferred from previous results. [16] Indeed, we already evidenced that similarly sized and similarly prepared iron oxide NPs are efficiently captured by HUVECs at 4 hours of contact. Moreover, we showed that the viability of these cells is weakly affected for NPs doses as high as 100 $\mu g.mL^{-1}$ for such short contact time. [16] In this context, we fixed the NPs dose to 50 $\mu g.mL^{-1}$, and we conducted magnetophoresis and XRF spectroscopy to determine the precise amount of loaded NPs by the cells (see experimental section) before submitting the studied cells to hyperthermia assay. The measured masses of iron averagely internalized in one cell of each cell line are given in Table 1.

A net discrepancy is observed between the values measured on HUVECs and U87-MGs, establishing that the malign cells are more sensitive to NPs than HUVECs and then they absorb larger amount of NPs (about twice). Besides, MTT assays were carried out on these incubated HUVEC and U87-MG cells to assess their viability in order to evidence any NP side effect before AMF application (Figure 5). They show that NPs have no significant effects at doses as high as 100 $\mu g.mL^{-1}$ for an incubation time of 4 hours. Typically, the viability of the cell lines is about 90 and 80%, respectively, while toxicity is considered when survival rate is below 80%.

	Magnetophoresis	XRF
	Iron quantity (pg/cell)	Iron quantity (pg/cell)
HUVEC	4.70 (0.77)	4.98 (1.97)
U87-MG	8.02 (0.84)	8.45 (3.34)

Table 1. Iron quantification (pg/cell) using magnetophoresis and XRF of HUVEC and U87-MG cells after 4 hours of γ-Fe_2O_3 NPs incubation (50 $\mu g.mL^{-1}$ in serum-free DMEM).

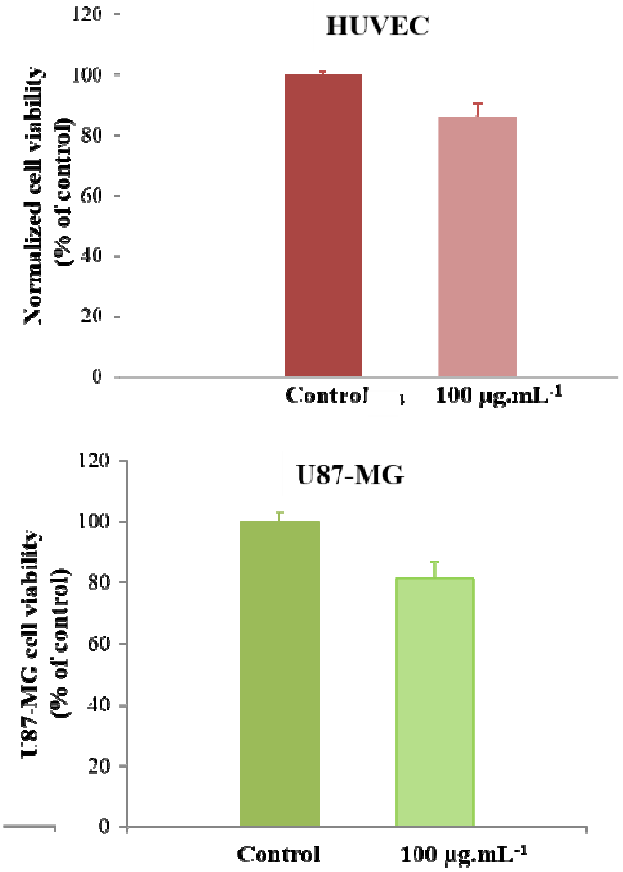

Figure 5. HUVECS (up) and U87-MGs (down) cell viability as inferred from MTT assays when exposed to γ-Fe_2O_3 NPs (100 $\mu g.mL^{-1}$ in serum-free DMEM) for 4 hours. Results are expressed as a ratio to non-stimulated serum-free cultured cells for each time point ($p<0.05$).

Finally, hyperthermia measurements were conducted on both cell lines incubated for 4 hours with a NPs dose of 50 µg.mL^{-1} and the initial linear rise in temperature versus time dependence was calculated by linear fit of the data points as illustrated in Figure 6. For the two cell lines, the temperature increases rapidly and reaches in a few seconds a maximal and stable value of 42°C. This value is clearly lower than that measured previously on NPs aqueous suspension, but sufficiently high to induce cell apoptosis and/or necrosis. Interestingly, the measured SAR value on U87-MGs appear to be higher than that obtained on HUVECs (Table 2).

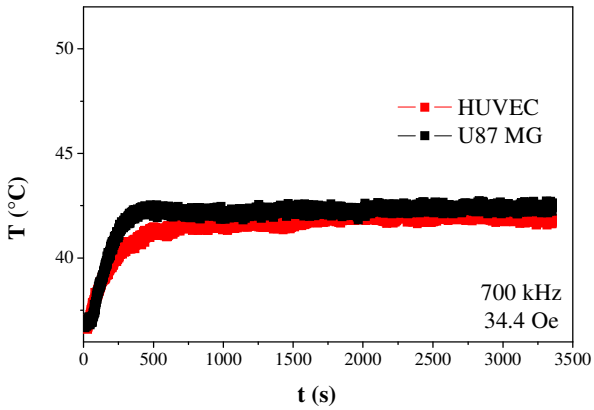

Figure 6. Temperature increase plotted as a function of time measured on HUVECs and U87-MGs incubated with γ-Fe_2O_3 NPs and exposed to a 700 kHz ac-magnetic field.

	HUVEC	U87-MG
Reached Temp. (°C)	42	42
SAR (W.g^{-1})	114(21)	178(37)

Table 2. Reached temperature and SAR measured on HUVECs and U87-MGs, after 4 hours of γ-Fe_2O_3 NPs incubation (50 µg.mL^{-1} in serum-free DMEM), when exposed to a 700 kHz ac-magnetic field.

To determine the effects of the observed heating on the cell viability, samples cell series were labeled by PI immediately after hyperthermia application to identify death cells and count them. The collected fluorescence images are given in Figure 7 in which dead cells appeared colored. By counting the fluorescent cells in visible light, the cell death rate (according to the total cells) was estimated. The mean cell death rate for each cell line is given in Figure 8 and compared to its value when the oscillating magnetic field is applied on the two cell lines without the presence of NPs (control). It appears clearly that the cell death is very weak without NPs, less than 10%, while it reaches 20 and 56% for NP incubated HUVECs and U87-MGs, respectively.

These treated cells were also observed by TEM to perceive the eventual morphological damages**.** The recorded micrographs (Figure 9) show a net cell alteration when the cells are subjected to the combined effect of NPs and AMF for both cell lines, with more dramatic effects on U87-MGs. Typically, the cell membrane integrity of U87-MGs and their fundamental organelles are significantly altered. Moreover, the images of NP incubated cells, compared to those of control, demonstrate that NPs are effectively internalized by the cells and concentrated within intracellular vesicles (the arrows in Figure 9).

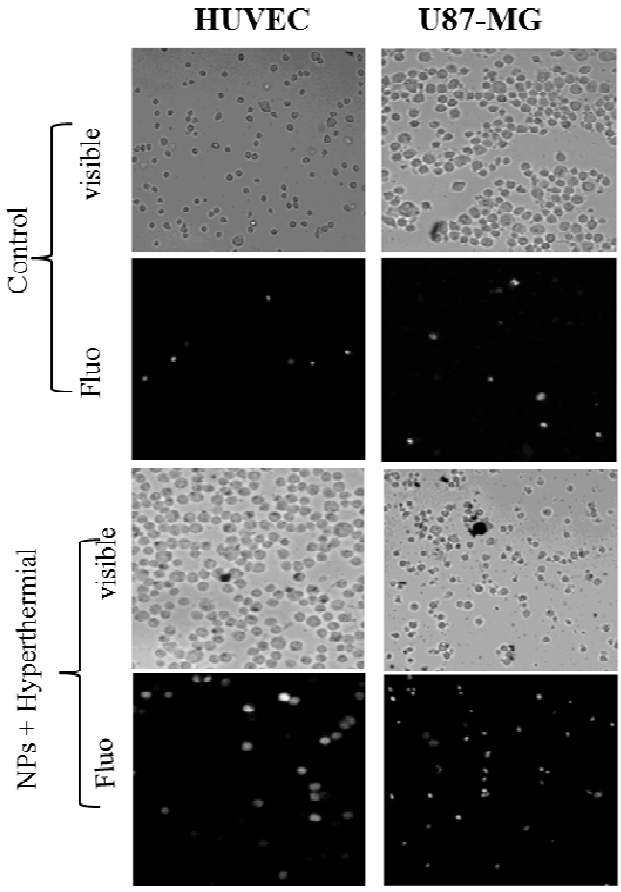

Figure 7. Fluorescence microscopy images after IP labeling of HUVECs and U87-MGs incubated with γ-Fe_2O_3 NPs and exposed to a 700 kHz ac magnetic field compared to those of the same cells exposed to the same magnetic treatment without NPs incubation.

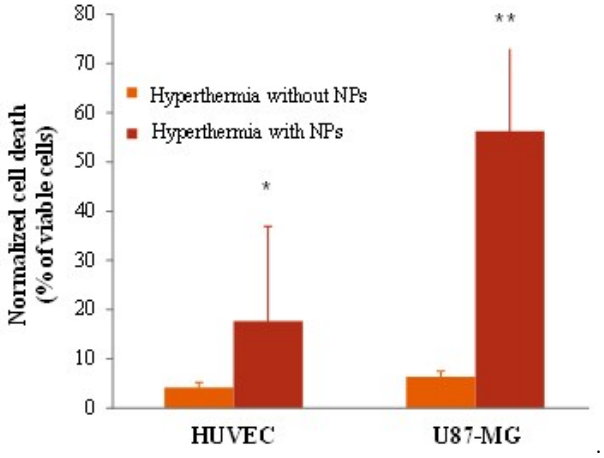

Figure 8. Result of death cell counting as monitored by IP assay. Results were expressed as a ratio to viable cells for each group (** p<0.01, * p<0.05).

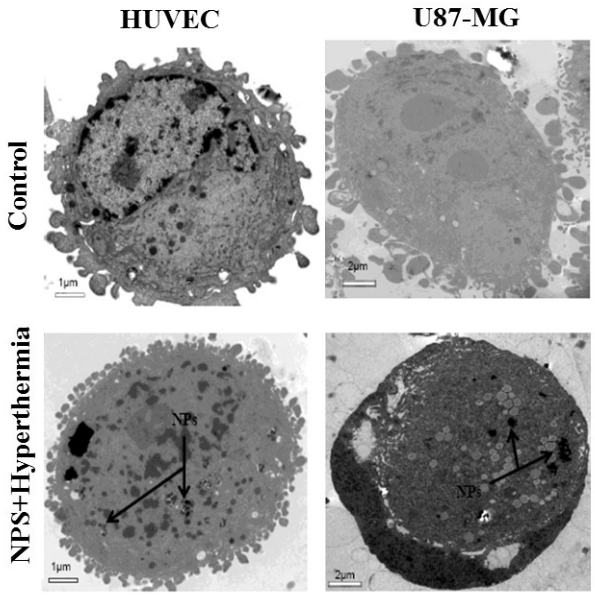

Figure 9. TEM micrographs recorded on HUVECs and U87-MGs exposed to hyperthermia after γ-Fe_2O_3 NPs incubation. Images were also recorded on the same cells free from NPs after the same magnetic treatment to serve as a control.

Discussion

In the present study, we investigate the effects of magnetic hyperthermia on HUVEC and U87-MG cells using superparamagnetic polyol-made 10 nm sized γ-Fe_2O_3 NPs and AMF. Our results showed that the application of magnetic hyperthermia during 1 hour on both cell lines was able to alter their viability and morphology. Many researches were focused on the characterization of iron oxide dedicated to hyperthermia application. [1,4-11] In the present investigation we used chemically stable, highly crystallized and monodispersed 10 nm sized [16] maghemite particles, almost free from organic coating and directly incubated with different cell lines and exposed to an alternating magnetic field of a frequency of 700 kHz and a magnitude of 34.4 Oe. Interestingly, the saturation magnetization of the NPs measured at +37°C, which corresponds to human body temperature, is relatively high compared to that reported for maghemite particles even with a larger size, when prepared by conventional soft chemistry methods (typically, aqueous precipitation). It is well known that physical and chemical properties of comparably-sized particles are significantly dependent upon their synthesis conditions. [12,24,25] Those related to the polyol process, namely forced hydrolysis of metallic salts in a relatively high boiling point polar solvent, a polyol, seem to be favorable for hyperthermia application.

We then examined the effect of γ-Fe_2O_3 NPs on each kind of cell line before AMF application using MTT assay. Note that, in the present case, the test was carried out with an automate. So it is considered more reliable than other tests such as Evan blue. Our data showed that cell viability ranged between 80% and 90% after 4 hours of incubation with NPs for doses as high as 100 µg.mL^{-1} (in free DMEM). It is commonly admitted that a MTT survival cell rate higher or equal to 80% means no toxic effect. [16,26] Clearly, iron oxide NPs failed to alter HUVECs and U87-MGs viability. Note that, by comparison, most of the cytotoxicity assays carried out on HUVEC and U87-MG cells incubated by differently sized and prepared iron oxide NPs show that HUVECs were non-altered for doses as high as 100 µg.mL^{-1} and short contact time [16,26] while U87-MGs were affected by accountable toxicity for doses close to 100 µg.mL^{-1} even for short contact time. [27] As far as we know the present study is the first contribution that evaluates viability of U87-MGs in contact with polyol-made γ-Fe_2O_3 NPs.

Before applying AMF for hyperthermia assay, the absorbed amount of γ-Fe_2O_3 NPs reached in each kind of cells, following a contact time of 4 hours, were determined. Based on magnetophoresis and XRF experiments, γ-Fe_2O_3 NPs appear to be efficiently up-taken by HUVEC and U87-MG cells. Minimum iron oxide concentration in cells is prerequisite for magnetic hyperthermia to tear down cells, particularly cancer cells. As well, the heat generation is directly dependent on the iron oxide quantity per cell. U87-MGs showed higher iron quantity per cell than HUVECs. Indeed, for a NP incubation dose of 50 µg.mL^{-1}, the measured iron mass per cell is of about 8 and 4 pg, respectively. Clearly, γ-Fe_2O_3 NPs were more efficiently internalized in U87-MGs than in HUVECs following 4 hours, leading to a higher in vitro SAR value in the former than in the latter.

Interestingly, previous investigations revealed significant iron oxide NPs loading up by HUVEC and/or U87-MG cells, forming clusters in cytoplasm, only for incubation times as high as 24 to 48 hours. [26,27] The observed NPs internalization for a contact time as short as 4 hours, in the present case, must be underlined.

Finally, cells were exposed to an alternating magnetic field of 34.4 Oe (23.10 kA.m^{-1}) amplitude and 700 kHz as frequency, for hyperthermia. The product (amplitude × frequency) is equivalent to about 1.50 × 10^{10} A.m^{-1}.s^{-1}. This value is slightly higher than the therapeutic limits used for hyperthermia treatment (5 × 10^9 A.m^{-1}.s^{-1}) [28] and those commonly used in preclinic assays. [7] The choice of such a field is based on the fact that relatively highly magnetized particles present a real capacity of heating under such magnetic field, [29] and the large amount of treated cells. This was verified in the present study by both SAR values and the reached temperature. SAR values of about 178 and 114 W.g^{-1} were measured on incubated HUVEC and U87-MG cells, respectively. These values are higher than that measured, 84 W.g^{-1}, on a concentrated aqueous suspension of NPs (20 g.L^{-1} compared to the 0.05 g.L^{-1} injected dose to the cells), in relation with cell confinement effects. Indeed, TEM observation of incubated cells evidenced net NPs charged lysosomes in cytoplasm, in both cell lines. In these vesicles, the local NPs concentration is usually very high [30] and through cooperative effects they generate more important heat, making them particularly valuable for cancer therapy by magnetic hyperthermia. Comparing the measured SAR values on our particles to those reported in the literature on some standards, typically, that of commercial iron oxide particles (FERIDEX), ours remained still competitive (84 W.g^{-1} versus 115 W.g^{-1} in distilled water). [31] FERRIDEX reference consists of 150 ± 30 nm sized Fe_3O_4 NPs prepared by aqueous co-precipitation, largely bigger than those studied here. For in vivo applications, restrictions upon NPs size

have to be seriously considered to promote their main biological barriers crossing. [32] Indeed NPs size may limit their diffusion into the whole body after intravenous injections. It may also affect their mutual magnetic interactions and then their aggregation. So highly magnetized small particles are more commonly preferred to larger ones. So even if in the present study all the magnetometry and magnetoclaorimetry investigation were performed on aggregated NPs, we already succeeded in producing stable colloid made from the dispersion of individual iron oxide particles functionalized by small hydrophilic molecules with an average hydrodynamic diameter of less than 50 nm. [32] The present results and the previous ones make us very confident for a future use of the produced NPs in *in vivo* conditions.

Temperature increase in both cell lines (+42°C) corresponded to the therapeutic temperature used for hyperthermia treatment. Hyperthermia activity is based on the fact that a temperature increasing between +41°C and +45°C can induce cell death. Particularly cancer cells are more sensitive to sudden increases in temperature than healthy surrounding cells. [33] Following 1 hour of alternating magnetic field application on about 10^6 cells, the temperature reached +42°C using our γ-Fe_2O_3 NPs at a concentration of 50 µg.mL^{-1}. Moreover, our results showed that this temperature increase led to cell death immediately after magnetic hyperthermia application. Indeed, we carried out PI assay which is known as a rapid and efficient test to check the cell viability. [22,34] We preferred to perform PI assay than MTT one after hyperthermia application. MTT requires cells processing (they have to be seeded in 96-well plates) which first need time and second might submit them to another kind of stress that might misled our final results. However, using PI we do not need to remove cells. PI penetrates quickly in cells after membrane damages. We obtain the results after only ten minutes. Moreover, necrosis induced by environmental disturbances violence often manifests immediately generalized swelling of intracellular organelles and rupture of membranes, while apoptosis induces, at the early stage, cell shrinkage. The cytoplasm becomes denser with tightly packed organelles. [35] PI assay coupled to TEM observation of the two types of cell lines evidenced that cell death triggered by γ-Fe2O3 NPs and AMF was mainly through necrosis. Similar cell death mechanism was observed in numerous magnetic hyperthermia investigations on malign cells, particularly glioma ones. [36] Comparing the cell death ratio, it appears that the single application of an AMF at 700 KHz for 1 hr was able to destroy 50% of U87-MG cells, when they were previously incubated by γ-Fe_2O_3 NPs for 4 hours at a relatively low dose (50 µg.mL^{-1}). In the same condition only 20% of HUVECs were affected most likely through necrosis process. The discrepancy of cell death ratio between the two cell lines is due to the fact that HUVECs are less sensitive than U87-MGs to the γ-Fe_2O_3 NPs assisted magnetic hyperthermia treatment. Such discrepancy between healthy and malign cells was already reported. [37]

Conclusion

Our investigation demonstrates the thermosensitivity of malign glioma (U87-MG) to magnetic hyperthermia. Whereby superparamagnetic polyol-made 10 nm sized γ-Fe_2O_3 NPs were used as heating sources. Two cell lines were submitted to NP mediated hyperthermia, healthy endothelial (HUVECs) and malign glioma (U87-MGs) ones. We demonstrate that the sensitivity of cell lines to short time hyperthermia application, in practice 1 hour, induces differently cell death most likely through necrosis process, when their temperature grow up to +42°C in a few seconds. In practice, more than 50% of U87-MG cells are destroyed in these conditions, while only 20% of HUVECs are. This discrepancy agrees with a higher thermosensitivity of malign cells compared to healthy ones. In the present case, it could be related to the ability of γ-Fe_2O_3 NPs to be more efficiently internalized in U87-MGs, leading to a final iron content per cell two time higher than in HUVECs, typically ~8 versus ~4 pg for NPs doses of 50 µg.mL^{-1} at 4 hours of time contact. These results are important, because they establish that γ-Fe_2O_3 NPs may be suitable for selective malign glioma tumor treatment as heating source under AMF conditions. *In vivo* assays on small mammals are planned to observe the overall effects of our NPs on living subjects and to confirm their efficiency in glioma therapy.

Acknowledgements

The authors are indebted to Pr. Jean-Paul Quisefit (Paris Diderot University) and Pr. Nicolas Menguy (Pierre & Marie Curie University) for their support during XRF and TEM experiments, respectively. They are also indebted to the French Foreign Minister for the A.H. PhD's grant (Eiffel program).

Notes and references

1 A. Jordan, A. P. Wust, H. Fahling, W. John, A. Hinz and R. Felix, *Int. J. Hyperthermia*, 1993, **9**, 51 ; S. Dutz, R. Müller, D. Eberbeck, I Hilger, M. Zeisberger, *Biomed. Eng. Biomed. Tech.*, 2015, **60**, 405 ; C. A. Quinto, P. Mohindra, S. Tong, G. Bao, *Nanoscale*, 2015, **7**, 12728..

2 M. Zeisberger, S. Dutz, R. Müller, R. Hergt, N. Matoussevitch and H. Bönnemann, *J. Magn. Magn. Mater*., 2007, **311**, 224 ; R. Hergt, R. Hiergeist, M. Zeisberger, D. Schüler, U. Heyen, I. Hilger and W. A. Kaiser, *J. Magn. Magn. Mater*., 2005, **293**, 80 ; B. Mehdaoui, A. Meffre, L. M. Lacroix, J. Carrey, S. Lachaize and M. Respaud, *J. Magn. Magn. Mater*., 2010, **322**, L49 ; L. M. Lacroix, R. B. Malaki, J. Carrey, S. Lachaize, M. Respaud, G. F. Goya and B. Chaudret, *J. Appl. Phys*., 2009, **105**, 023911.

3 N. K. Prasad, L. Hardel, E. Duguet and D. Bahadur, *J. Magn. Magn. Mater*., 2009, **321**, 1490 ; S. Vasseur, E. Duguet, J. Portier, G. Goglio, S. Mornet, E. Hadova, K. Knížek, M. Maryško, P. Veverka and E. Pollert, *J. Magn. Magn. Mater*., 2006, **302**, 315 ; S. Vasseur, E. Duguet, J. Portier, G. Goglio, S. Mornet, E. Hadova, K. Knížek, M. Maryško, P. Veverka and E. Pollert, *J. Magn. Magn. Mater*., 2006, **302**, 315 ; J. P. Fortin, F. Gazeau and C. Wilhelm, *Eur Biophys. J*., 2008, **37**, 223 ; Z. Beji, A. Hanini, L. S. Smiri, J. Gavard, K. Kacem, F. Villain, J. M. Grenèche, F. Chau and S. Ammar, *Chem. Mater*., 2010, **22**, 420 ; P. Pradhan, J. Giri, G. Samanta, H. DevSarma, K. P. Mishra, J. Bellare, R. Banerjee and D. Bahadur, *J Biomed Mater. Res. B: Appl. Biomater*., 2006, **81**, 12.

4 J. P. Fortin, C. Wilhelm, J. Servais, C. Ménager, J. C. Bacri and F. Gazeau, *J. Am. Chem. Soc*., 2007, **129**, 2628.

5 L. Lartigue, P. Hugounenq, D. Alloyeau, S. P. Clarke, M. Lévy, J. C. Bacri, R. Bazzi, D. F. Brougham, C. Wilhelm and F. Gazeau, *ACS Nano*, 2012, **6**, 10935
6 H. M. Fan, J. B. Yi, Y. Yang, K. W. Kho, H. R. Tan, Z.X. Shen, J. Ding, X. W. Sun, M. C. Olivo and Y. P. Feng, *ACS Nano,* 2009, **3**, 2798.
7 A. Jordan, R. Scholz, K. Maier-Hauff, M. Johannsen, P. Wust, J. Nadobny H. Schirra and H. Schmidt, *J. Magn. Magn. Mater*., 2001, **225**,118 ; b) K. Maier-Hauff, F. Ulrich, D. Nestler, H. Niehoff, P. Wust, B. Thiesen, H. Orawa, V. Budach and A. Jordan, *J. Neurooncol*., 2011, **103**, 317.
8 C. Wilhelm, J. P. Fortin and F. Gazeau, *J. Nanosci. Nanotechnol*., 2007, **7**, 2933 ; S. Laurent, S. Dutz, U. O. Häfeli and M. Mahmoudi, *Adv. Colloid Interface Sci*., 2011, **166**, 8 ; S. Mornet, S. Vasseur, F. Grasset and E. Duguet, *J. Mater. Chem*., 2004, **14**, 2161 ; W. Wu, Q. He and C. Jiang, *Nanoscale Res. Lett*., 2008, **3**, 397.
9 P. Hugounenq, M. Levy, D. Alloyeau, L. Lartigue, E. Dubois, V. Cabuil, C. Ricolleau, S. Roux, C. Wilhelm, F. Gazeau and R. Bazzi*, J. Phys. Chem. C*, 2012, **116**, 15702.
10 M. Comes Franchini, G. Baldi, D. Bonacchi, D. Gentili, G. Giudetti, A. Lascialfari, M. Corti, P. Marmorato, J. Ponti, E. Micotti, U. Guerrini, L. Sironi, P. Gelosa, C. Ravagli, A. Ricci Small, 2010, 6, 366 ; b) G. Baldi, C. Ravagli, F. Mazzantini, G. Loudos, J. Adan, M. Masa, D. Psimadas, E. A. Fragogeorgi, E. Locatelli, C. Innocenti, C. Sangregorio and M. Comes Franchini, *Int. J. Nanomedicine*, 2014, **9**, 3037.
11 S. Ammar, A. Helfen, N. Jouini, F. Fiévet, I. Rosenman, F. Villain and P. Molinié, *J. Mater. Chem*., 2001, **11**, 186 ; H. Basti, A. Hanini, M. Levy, L. Ben Tahar, F. Herbst, L. S. Smiri, K. Kacem, J. Gavard, C. Wilhelm, F. Gazeau, F. Chau and S. Ammar, *Mater. Res. Express*, 2014, **1**, 045047.
12 S. Ammar, A. Helfen, N. Jouini, F. Fiévet, I. Rosenman, F. Villain, P. Molinié and M. Danot, *J. Mater. Chem*., 2001, **11**, 186 ; S. Chkoundali, S. Ammar, N. Jouini, F. Fiévet, M. Richard, P. Molinié, F. Villain and J. M. Grenèche, *J. Phys.: Condens. Matter*, 2004, **16**, 4357 ; S. Ammar, N. Jouini, F. Fiévet, Z. Beji, L.S. Smiri, P. Molinié and J. M. Grenèche, *J. Phys.: Condens. Matter*, 2006, **18**, 9055 ; H. Piraux, J. Hai, S. Ammar, F. Gazeau, T. Gaudisson, J. M. El Hage Chahine and M. Hémadi, *J. Appl. Phys*., 2015, **117**, 17A336.
13 C. Wilhelm, J. P. Fortin and F. Gazeau, *J. Nanosci. Nanotechnol.*, 2007, **7**, 2933 ; K. Buyukhatipoglu and A. M. Clyne, *J. Biomed. Mater. Res. A*, 2011, **96**, 186.
14 A. C. Silva, T. R. Oliveira, J. B. Mamani, S. M. Malheiros, L. Malavolta, L. F. Pavon, T. T. Sibov, E. Amaro Jr, A. Tannús, E. L. G. Vidoto, M. J. Martins, R. S. Santos and L. F. Gamarra, *Int. J. Nanomedicine*, 2011, **6**, 591 ; S. A. Meenach, J. Z. Hilt and K. W. Anderson, *Acta Biomater*., 2010, **6**, 1039 ; M. Shinkai, M. Yanase, H. Honda, T. Wakabayashi, J. Yoshida and T. Kobayashi, *Jpn. J. Cancer Res*., 1996, **87**, 1179.
15 H. Basti, L. Ben Tahar, L. S. Smiri, F. Herbst, M. J. Vaulay, F. Chau, S. Ammar and S. Benderbous, *J. Colloid Interface Sci*., 2010, **341**, 248.
16 A. Hanini, A. Schmitt, K. Kacem, F. Chau, S. Ammar and J. Gavard, *Int. J. Nanomedicine*, 2011, **6**, 787.
17 C. J. S. Edgell, C. C. McDonald and J. B. Graham, *Proc. Natl. Acad. Sci. USA*, 1983, **80**, 3734.
18 M. J. Clark, N. Homer, B. D. O'Connor, Z. Chen, A. Eskin, H. Hane Lee, B. Merriman and S. F. Nelson, *PLoS Genetics*, 2010, **16**, e1000832.
19 C. Wilhelm, F. Gazeau and J. C. Bacri, *Eur. Biophys. J*., 2002, **31**, 118.
20 J. P. Fortin, C. Wilhelm, J. Servais, C. Menager, J. C. Bacri, F. Gazeau, *J. Am. Chem. Soc*., 2007, **129**, 2628.
21 I. Hilger, K. Frühauf, W. Andrä, R. Hiergeist, R. Hergt and W. A. Kaiser*, Acad. Radiol*., 2002, **9**, 198 ; X. L. Liu, E. S. G. Choo, A. S. Ahmed, L. Y. Zhao, Y. Yang, R. V. Ramanujan, J. M. Xue, D. D. Fan, H. M. Fan and J. Ding, *J. Mater. Chem. B*, 2014, **2**, 120.
22 G. Beaune, M. Levy, S. Neveu, F. Gazeau, C. Wilhelm, C. Ménager, *Soft Matter*, 2011, **7**, 6248 ; b) P. Guardia R. Di Corato, L. Lartigue, C. Wilhelm, A. Espinosa, M. Garcia-Hernandez, F. Gazeau, L. Manna, T. Pellegrino, *ACS Nano*, 2012, **6**, 3080.
23 S. Mornet, S. Vasseur, F. Grasset and E Duguet, *J. Mater. Chem*., 2004, **14**, 2161 ; E. M. Múzquiz-Ramosa, V. Guerrero-Cháveza, B. I. Macías-Martíneza, C. M. López-Badilloa, L. A. García-Cerdab, *Ceram. Int*., 2015, **41**, 397 ; E. Garaio , O. Sandre, J. M. Collantes, J. A. Garcia, S. Mornet and F. Plazaola, *Nanotechnol.,* 2015, **26**, 015704.
24 M. P. Gonzalez-Sandoval, A. M. Beesley, M. Miki-Yoshida, L. Fuentes-Cobas and J. A. Matutes-Aquino, *J. Alloys Compds*., 2004, **369**, 190 ; J. Lee, T. Isobe and M. Senna, *J. Colloid Interface Sci*., 1996, **177**, 490.
25 W. Wu, Q. He, C.-Z. Jiang, *Nanoscale Res. Lett*., 2008, **3**, 397.
26 O. Masala, R. Seshadri, *J. Am. Chem. Soc*., 2005, **127**, 9354 ; S. Martins, S. Costa-Lima, T. Carneiro, A. Cordeiro-da-Silva, E. B. Souto and D. C. Ferreira, *Int. J. Pharm*., 2012, **430**, 216 ; N. Ignjatović, Z. Ajduković, V. Savić, S. Najman, D. Mihailović, P. Vasiljević, Z. Stojanović, V. Uskoković and D. Uskoković, *J. Mater. Sci. Mater. Med.*, 2013, **24**, 343.
27 T. Schlorf, M. Meincke, E. Kossel, C. C. Glüer, O. Jansen and R. Mentlein, *Int. J. Mol. Sci*., 2010, **12**, 12.
28 B. Ankamwar, T. C. Lai, J. H. Huang, R. S. Liu, M. Hsiao, C. H. Chen and Y. K. Hwu, *Nanotechnol.*, 2010, **21**, 75102.
29 W. J. Atkinson, I. A. Brezovich, D. P. Chakraborty, *IEEE Trans Biomed Eng*., 1984, **31**, 70.
30 A. G. Kolhatkar, A. C. Jamison, D. Litvinov, R. C. Willson and T. R. Lee, *Int. J. Mol. Sci*., 2013, **14**, 15977.
31 Y. Okuhata, *Adv. Drug. Delivery Rev*., 1999, **37**, 121.
32 J. Fouineau, K. Brymora, L. Ourry, N. Yaacoub, F. Mammeri, F. Calvayrac, S. Ammar and J. M. Grenèche, *J. Phys. Chem. C,* 2013, **117**, 14295 ; K. Brymora, J. Fouineau, , F. Chau, N. Yaacoub, J. M. Grenèche, J. Pinson, S. Ammar and F. Calvayrac, *J. Nanopart. Res.*, 2015, **17**, 438 ; H Basti, L. Ben Tahar, L. S. Smiri, F. Herbst, S. Nowak, C. Mangeney and S. Ammar, *Colloids Surf. A*, 2016, **490**, 222.
33 R. Cavaliere, E. C. Ciocatto, B. C. Giovanella, C. Heidelberger, R. O. Johnson, M. Margottini, B. Mondovi, G. Moricca and A. Rossi-Fanelli, *Cancer*, 1967, **20**, 1351 ; J. Overgaard, *Cancer*, 1977, **39**, 2637 ; J. van der Zee, *Ann Oncol*., 2008, **13**, 1173.
34 T. Fernandez Cabada, C. S. de Pablo, A. M. Serrano, P. Guerrero Fidel, J. J. Olmedo and M. R. Gomez, *Int. J. Nanomed*., 2012, **7**, 1511.
35 S. Elmore, *Toxicol. Pathol*., 2007, **35**, 495.
36 A. Ito, M. Shinkai, H. Honda, T. Wakabayashi, J. Yoshida and T. Kobayashi, *Cancer Immunol. Immunother*., 2003, **52**, 80.
37 T. Komata, T. Kanzawa, T. Nashimoto, H. Aoki, S. Endo, M. Nameta, H. Takahashi, T. Yamamoto, S. Kondo and R. Tanaka, *J. Neuro-Oncol*., 2004, **63**, 10.

Thermosensitivity profile of malign glioma U87-MG cells and human endothelial cells following γ-Fe_2O_3 NPs internalisation and magnetic field application.